DSC-Vol. 58, Proceedings of the ASME Dynamics Systems and Control Division
ASME 1996

A Non-Linear Wheelset Model to Predict Derailment

Imtiaz Haque*, Patrick McGirt*, and Mark L. Nagurka**
* Clemson University, Clemson, South Carolina
** Carnegie Mellon Research Institute, Pittsburgh, Pennsylvania

ABSTRACT

The performance of a rail vehicle is a direct function of the ability of its wheelsets to negotiate the track. This paper presents the results from a detailed dynamic simulation study of wheelset motions with special emphasis on safety-related behavior. The wheelset is assumed to maintain continuous wheel-rail contact as it traverses smooth track that may be tangent or curved, and rigid or flexible. The model accounts for nonlinearities due to wheel-rail profile geometry and friction (creep) force and the longitudinal translation of the contact patch as a function of wheelset yaw angle. The results demonstrate non-linear features, such as limit cycles, and extremes of behavior including wheel-lift, and wheel-climb. The model has also been exercised to generate steady-state force and moment characteristics.

INTRODUCTION

The advent of high speed rail vehicle systems necessitates the development of computer tools for accurate safety assessment. The high speeds of operation of such systems demand that the modeling capability be able to predict a wide range of dynamic behavior including loss of guidance (derailment), ride quality, and structural integrity. Since the wheelset is the fundamental element of a railway vehicle, the development of an accurate model that captures the key characteristics of wheelset physical behavior is of paramount interest.

Numerous analytic models have been developed to predict wheelset behavior. A summary of earlier efforts is reported by Karmel and Sweet (1982). Improvements in contact modeling features such as two-point contact have made their way into current popular multi-body simulation packages (Kortum and Sharp, 1993). The models developed differ in many ways including the degrees of freedom, creep force formulations, the numerical algorithms (implemented to solve the single-point and two-point contact problems, and for numerical integration). However, the models have rarely been exercised to simulate extremes of wheelset behavior such as wheel-climb and wheel-lift. In general, the effect of model differences on such predictions is unknown. One noteworthy effort to understand the mechanism of wheelset derailment using a dynamic wheelset model was that of Karmel and Sweet (1982). Their model was developed for single point contact on rigid tangent track. Karmel and Sweet correlated the results of their model with scaled model tests in the laboratory.

The prediction of wheel-climb and wheel-lift involves the ability to simulate amplitudes of wheelset motions that are quite large, and requires a non-linear dynamic model. The non-linear effects of the creep forces and the wheel-rail geometry become highly pronounced in conditions of severe flange contact. Combined with the high speed operation, the non-linear effects produce results that are distinct from tread contact/low speed operations (Karmel and Sweet, 1982).

In the study presented here, a detailed wheelset model developed by Nagurka (1983) has been adapted for predicting wheel-climb and wheel-lift. The model includes the lateral, yaw, and spin degrees of freedom as well as non-linear wheel-rail geometry, non-linear creep force characteristics, and laterally flexible rails. In addition to the lateral and yaw motions, the spin, as measured by the deviation of the rolling velocity from the nominal value, is essential in a wheelset model that predicts derailment. (During steady flange contact, the axle spin can drop by about 3% thereby having a significant effect on the longitudinal creep forces (Sweet and Sivak, 1979)). This paper demonstrates some of the capabilities of Nagurka's model in predicting behavior during extreme flanging/derailment and force-moment characteristics during steady-state operations.

WHEELSET MODELING

A detailed derivation of the wheelset model is given by Nagurka (1983). Important features of the model are as follows:

1. In the general case, the wheelset is navigating a changing radius right hand curve with a changing superelevation.
2. The track is assumed to be smooth.
3. The wheelset remains in contact with the rail at all times. Wheel-lift is assumed when one of the normal forces goes to zero.
4. Kinematic constraint equations due to wheel-rail contact. are used to calculate wheelset vertical and roll velocities.
5. Two point contact is possible on either wheel.
6. The contact point on the wheel translates longitudinally with yaw angle of the wheelset.
7. Each rail is modeled as an effective mass, spring and damper with a lateral degree of freedom.
8. The creep forces are modeled using an approximation to Kalker's non-linear creep theory (Kalker, 1968) based on Vermeulen and Johnson's work (1965). This approach, known as the Modified Vermeulen-Johnson (MVJ) Theory includes the effect of spin creep (Nagurka, 1983).
9. The normal force equations contain the influence of the roll and vertical accelerations.
10. The equations of motion retain non-linear kinematic quantities and gyroscopic terms.

Solution techniques for the wheelset equations have also been outlined by Nagurka (1983).

The wheelset equations and the associated solution methods have been converted into computer programs written in FORTRAN for both steady-state and time domain solutions. A Runge-Kutta-Fehlberg routine (Forsythe, et.al., 1977) with a variable time step is used to integrate the equations of motion for the dynamic simulation. The normal forces are implicitly

contained in the creep forces that appear in the equations of motion.

The program iterates and solves the normal force equations within a given time step, and then integrates the equations of motion.

The inputs are the inertial parameters of the wheelset, external wheel loads or suspension forces between the wheelset and the truck and a specified load at the wheelset cg, friction coefficients on the tread and the flange, and the wheel-rail geometry parameters, namely, rolling radii, contact and roll angles, and curvatures as functions of wheelset lateral displacement. The wheel-rail geometry parameters are read in as tables. Also input is the rail effective mass, damping and stiffness along with the flange clearance. Outputs from the program consist of all the wheel-rail states and forces, L/V ratios at each wheel, and the normalized lateral force (Total Lateral Force/Lateral Axle Force for Cylindrical Wheels in Full Slip) and normalized yaw moment (Total Yaw Moment/Limiting Yaw Moment for Cylindrical Wheels in Full Longitudinal Slip).

The steady-state program neglects the dynamic terms in the equations of motion. It iterates on the normal force equations and solves the steady-state equations for the variables of interest. For the two-point contact problem on rigid rail, the program requires the input of a lateral force which allows one to use the wheelset lateral, roll, and vertical equations to solve for the normal forces at contact. In contrast some researchers use a heuristic distribution of load between flange and tread based on the lateral position of the wheelset in the two-point contact region (NUCARS, 1993). This approximation allows them to avoid the iteration within the time step that is required to accurately solve for the normal forces between the wheel and the rail. For flexible rail, the problem is determinate. The inputs to this program consist of the wheelset lateral displacement and yaw angles, the wheel loads, the coefficient of friction on the flange and the tread, the flange clearance, the rail stiffness and the wheel-rail geometry. The outputs from the program consist of the spin equilibrium velocity, creep and normal forces, L/V ratios at each wheel, and the normalized lateral force and yaw moment defined above.

RESULTS

Wheelset Dynamic Behavior

The wheelset parameters are shown in Table 1. The results are for a free wheelset, i.e. a wheelset that is unrestrained. Two different configurations are presented. The first is a wheelset loaded at its cg with an external load and the second is a wheelset with a fixed vertical load on each wheel. The results show some of the important behavioral characteristics of the wheelset during wheel-climb and wheel-lift without the complications of having the influence of truck design in the model.

The dynamic results are for tangent track. Similar results can be obtained for curved track. To remove the influence of the rail model, a rigid rail is used. Two-point contact on rigid rail during dynamic operating conditions implies that the wheelset lateral velocity is zero. This leads to extremely high contact forces, resulting in numerically unstable results. Hence, the two-point contact capability has been disabled for these cases. The results shown below predict the following:

1. Wheelset limit cycle behavior
2. Wheelset behavior during wheel-climb

Wheelset Limit Cycle Behavior. Perhaps the most interesting dynamic aspect is that of stability of wheelset motions. Linear analysis shows the existence of a critical speed below which oscillations decay and above which they grow. However, non-linearities strongly modify this behavior. Non-linear behavior is known to include stable and unstable limit cycles with initial conditions determining their occurrence (Law, Haque, and Cooperrider, 1991). Stable limit cycles exist due to the large stabilizing forces generated by the wheel flanges. At higher amplitudes the flange is unable to provide the restoring forces needed to curtail the motion and derailment is predicted. Table 2 shows stable limit cycle amplitude versus speed for a limited number of speeds and initial amplitudes close to flanging. The results show stable limit cycle behavior much below and above the predicted linear critical speed of 3.35 m/sec. In addition, the amplitude is a function of forward speed. Very small initial amplitudes at the higher speeds cause wheelset motions to increase rapidly resulting in unstable wheelset behavior. These effects are more pronounced with wheel-rail geometry that is non-linear in the tread region.

Wheel-lift occurs when the wheelset flange impacts the rail at a relatively high lateral velocity causing the non-flanging wheel to lift off the rail. Forward speed is an important parameter in wheel-lift. The same set of initial conditions at higher speeds can lead to derailment due to either wheel-lift or wheel-climb. Figure 1 shows the wheelset lateral displacement at a speed of 30 m/sec with an external load of 72,280 N. The wheelset exhibits stable limit cycle behavior as is to be expected with flange contact occurring at both wheels at the extremes of motion (solid line in figure). An increase in speed to 35 m/sec results in wheel-lift with the normal force on the non-flanging wheel going to zero (dashed line in figure) at 0.6 sec. Linear analysis predicts a hunting frequency for this model of approximately 2 Hz. The figure shows that for the initial stages of motion, where the contact is still on the tread, the frequency of oscillation is approximately that predicted by the linear analysis but as the amplitude grows and flange contact occurs, the frequency changes and becomes amplitude dependent.

Figure 2 shows the wheelset yaw angle versus wheelset lateral displacement. Wheelset yaw motions are out of phase with lateral displacement and the effect of flange contact is to skew the plot. The steering effect of the flange is evident in the plot as the wheelset yaws back to the track center in flange contact.

Figure 3 is a phase-plane plot with stable limit cycle behavior being evident. The wheelset reverses its lateral velocity with very little change in position. The dips in wheelset velocity occur when the wheelset moves off the flange and onto the tread resulting in lower roll and vertical accelerations. The subsequent increase in wheelset velocity is due to the lateral forces on the wheelset.

Figure 4 shows large excursions in the normal forces at flanging. This is due to the rapid deceleration of the wheelset because of the large contact angles at the flange. The forces on the left and right wheels have similar characteristics and magnitudes. These forces provide the lateral forces that return the wheelset back to the track center. The L/V ratios (Figure 5) at flanging approach Nadal's limit and decrease as the wheelset moves back towards the center of the track. They demonstrate the same trends as for the normal forces. A three-dimensional plot of the normalized lateral force versus the normalized yaw moment and the wheelset lateral displacement (Figure 6) shows some interesting features. For wheelset displacements resulting in contact on the tread, the lateral force and yaw moment remain fairly small with more extreme values prevalent at flange contact. The sensitivity of the force and moment relationships to wheelset motion at the flange is evident from the plot. This force characteristic is also sensitive to the modeling of the transition from the tread to the flange.

A drop in axle speed (not shown here) when the wheelset encounters the flange results in an unbalance in the longitudinal creep forces which exert a yaw moment that brings the wheelset back to the center.

From the simulation studies, it is noted that:

1. For tangent track operation with an external load applied to the wheelset cg, the mode of derailment experienced is wheel-lift. When the wheelset forward velocity is high enough and flanging occurs on one wheel, the non-flanging wheel loses contact with the rail and the wheelset rolls over. Although the study only considers a free wheelset (which has an increased propensity to lift), the phenomenon of wheel-lift has been observed in the field during hunting. The model appears to faithfully mimic that behavior.

2. The effect of the roll and vertical accelerations on the speed at which wheel-lift occurs is significant and the inclusion of these terms is important. Neglecting these effects leads to a much higher speed at which this mode of derailment occurs.

Wheelset Behavior During Wheel Climb. To demonstrate wheel-climb on tangent track, the model was run at different speeds with a constant vertical load on each wheel. This prevents wheel-lift from occurring and the wheelset readily exhibits wheel-climb (Figure 7). The simulation is stopped when the wheelset lateral displacement exceeds the limits of the data table (wheelset contact is on the crown of the flange). The predictions match results observed by Karmel and Sweet (1982). The wheelset climbs the flange a number of times, each time dropping down and then it suddenly derails. The derailment occurs very rapidly as the wheelset traverses up the flange and contact exceeds that part of the flange where the contact angle is a maximum (wheelset lateral translation = 0.009 m). Figures 8, and 9 demonstrate other characteristics during this mode of wheelset behavior. The normal forces on the left and right wheels show different magnitudes during flanging with the magnitudes progressively growing (Figure 8) until the moment of derailment when the normal force shows a small decrease. This is because as the wheelset approaches wheel-climb, the lateral creep force on the flanging wheel produces a moment (limited by the decreasing normal force at the flange) that tends to unload the wheelset. The lateral creep force at the non-flanging wheel continues to provide a roll moment and lateral force that leads to wheel-climb. The magnitudes of the normal forces and their characteristics are strongly influenced by the wheelset states and the contact geometry. Just before derailment the normal force falls rapidly because the contact angle diminishes as the wheelset climbs onto the crown of the wheel. This has been noticed in tests by the Japanese National Railways (Matsudaira and Yokose, 1962). After flange contact the axle speed drops as the wheelset climbs the rail (Figure 9).

Wheelset Steady-State Behavior.

The behavior of this model in steady-state has been documented by Haque and Nagurka (1995). For steady-state the wheelset equations are independent of speed if the model is run at balance speed. The two regimes of operation, namely single and two-point contact, are included in the model. The steering characteristics on tangent and curved track are presented.

Steering Characteristics. The steady-state steering characteristics were evaluated for several axle positions including the wheelset centered on the track, the wheelset displaced in tread contact, and the wheelset fully in flange contact. The model exhibits typical lateral and longitudinal force behavior. Figures 10 and 11 show the normalized yaw moment plotted versus the normalized lateral force for a wheelset on both tangent and curved track. Two different lateral displacements are considered, one with contact on both left and right wheels on the tread and the other with contact on the tread and the left wheel flange. Figure 10 shows the influence of rolling line offset on the creep characteristics with the yaw moments showing opposite signs for tangent versus curved track and the restoring moment increasing with tighter curves. In Figure 11 it is observed that for tangent track, the sign of the yaw moment for the flange case is the same as that for the tread but the values of lateral force and moment are higher. Therefore, an outward motion of the wheelset results in forces which tend to bring the wheelset back to the center of the track. In the case of curved track, for contact on the tread, the tendency of the wheelset is to keep moving in a straight line. For contact wheelset is to keep moving in a straight line. Contact on the flange reverses the sign of the yaw moment, indicating the tendency of the wheelset to follow the track curvature. Also, for the case of flange contact, the normalized axle lateral force considerably exceeds the limiting friction value, a result of the high normal force due to the large contact angle.

SUMMARY

In summary, a detailed non-linear model has been presented for predicting wheelset behavior in the context of safety related studies of railway vehicles. The model has been used to simulate behavior during wheel-climb and wheel-lift and steady-state characteristics have been determined. The model has lateral, yaw and spin degrees of freedom and has the capability to represent single-point and two-point contact as well as transitions from one to the other. Results obtained with the model show strong correlation with previous work (Haque and Nagurka, 1995). Current work involves the inclusion of beam-

on-elastic-foundation rail model as well as modeling the impact between wheel and rail at the onset of flanging.

DEDICATION

This work is dedicated to the memory of Mr. Donald Ahlbeck of Battelle Laboratories, a valued colleague whose insights on rail vehicle behavior marveled those of us less gifted. Don's passing in December 1995 was a great loss to the railroad research community.

ACKNOWLEDGMENT

The authors also wish to thank Dr. Herb Weinstock and Mr. Dave Tyrell (Volpe National Transportation Systems Center, Cambridge, MA) and Mr. Jeff Hadden, Mr. Jim Tuten, and Mr. Richard Rice (Battelle Laboratories, Columbus, OH) for their interest in this work. Mr. Manish Shah's manuscript preparation efforts are also gratefully acknowledged.

REFERENCES

Cooperrider, N. K., Law, E. H., Hull, R., Kadala, P. S., and Tuten, J. M., 1975, " Analytic and Experimental Determination of Nonlinear Wheel-Rail Geometric Constraints," FRA Report No. FRA/ORD-76/244.

Forsythe, G. E., Malcolm, M.A., and Moler, C., 1977, Computer Methods for Mathematical Computations, Prentice Hall.

Haque, I., and Nagurka, M. L., 1995, "Wheel/Rail Interaction Model Comparisons," Report No: TTD No. VA-3204, Contract No. DTRS-57-93-D-0027.

Kalker, J. J., 1979, "A Survey of Wheel-Rail Rolling Contact Theory," Vehicle System Dynamics, Vol. 8, No. 4, pp 317-358.

Kalker, J. J., 1982, "A Fast Algorithm for the Simplified Theory of Rolling Contact," Vehicle System Dynamics, Vol. 11, pp. 1-13.

Karmel, A. and Sweet, L. M., 1982, "Wheelset Mechanics During WheelClimb Derailment," ASME Symposium on Computational Methods in Ground Transportation Vehicles, M. M. Kamal and J. A. Wolf Editors, pp. 201-216.

Kortum, W. and Sharp, R. S., 1993, "Multi-body Computer Codes for Vehicle System Dynamics," Supplement to Vehicle System Dynamics, Vol. 22.

Nagurka, M. L., 1983, "Curving Performance of Rail Passenger Vehicles," Ph.D. Thesis, Department of Mechanical Engineering, M.I.T.

Sweet, L. M., and Sivak, J. A., 1979, "Non-Linear Wheelset Forces in Flange Contact-Part 1: Steady State Analysis and Numerical Results," ASME Journal of Dynamic Systems, Measurements, and Control, Vol. 101.

Vermeulen, P. J. and Johnson, K. L., 1964, "Contact of Non-spherical Elastic Bodies Transmitting Tangential Forces," Transactions of the ASME, pp. 338-340.

Table 1: Simulation Data

Wheelset Mass	1751 kg
Spin Moment of Inertia	200 kg-m^2
Yaw Moment of Inertia	761 kg-m^2
Mean Rolling Radius	0.42 m
Rail Profile	1938 N/m New Rail
Wheel Profile	AAR 1:20 New Wheel
Coefficient of Friction	0.375
Flange Clearance	0.008 m

Table 2: Stable Limit Cycle Amplitude Versus Speed

Speed m/sec	Limit Cycle Amplitude mm
30.0	8.122
27.5	8.100
25	8.079
22.5	8.061
20.0	8.044
15.0	8.020
2.0	7.900

Note: Linear Critical Speed = 3.35 m/s

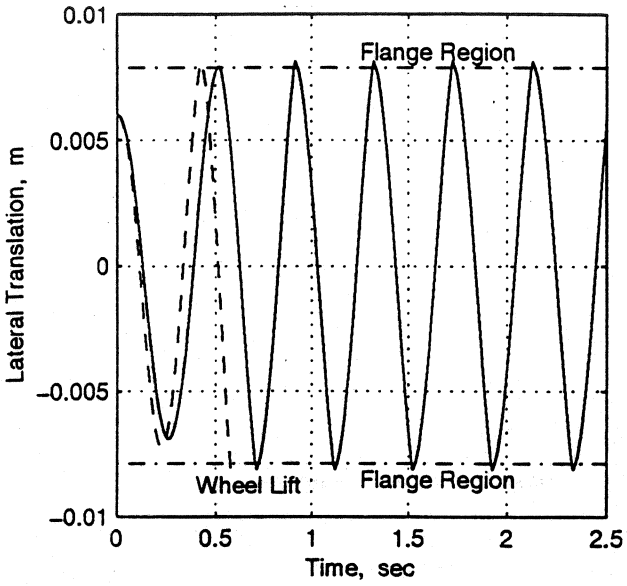

Figure 1. Wheelset Lateral Response (Solid Line ~ 30 m/sec, Dashed Line ~ 35 m/sec)

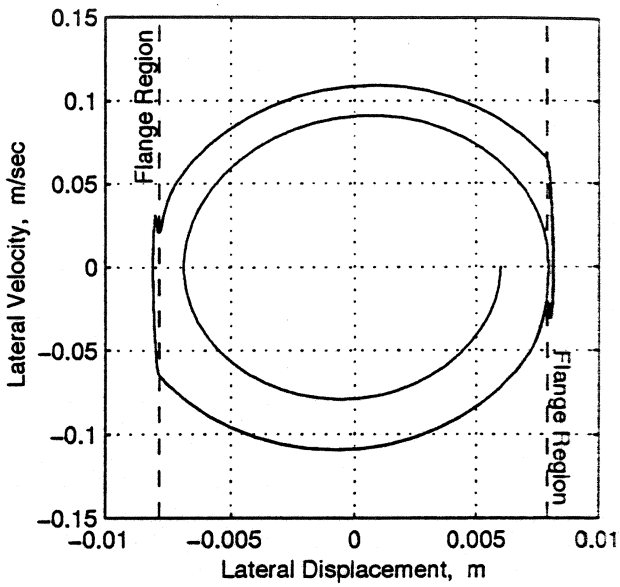

Figure 3. Wheelset Lateral Velocity vs Lateral Displacement (V = 30 m/sec)

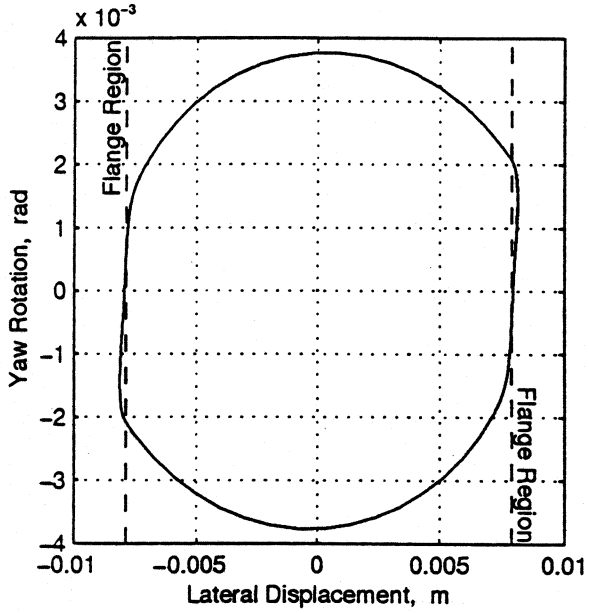

Figure 2. State Space Plot: Wheelset Yaw vs Lateral Displacement (V = 30 m/sec)

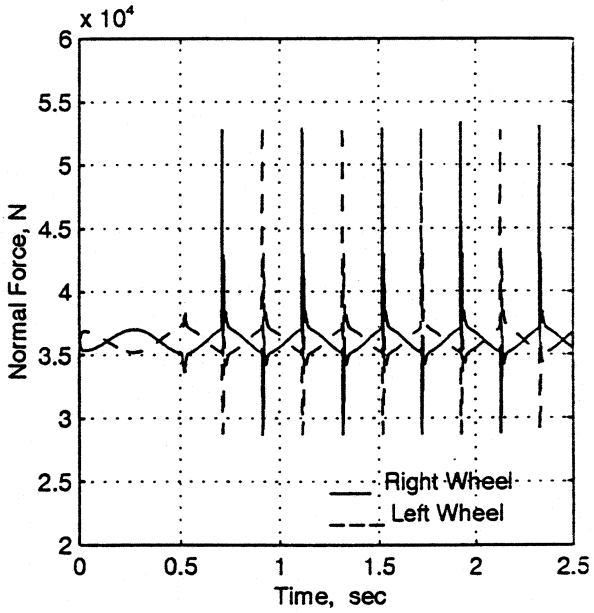

Figure 4. Normal Forces at the Left and Right Wheel (V = 30 m/sec)

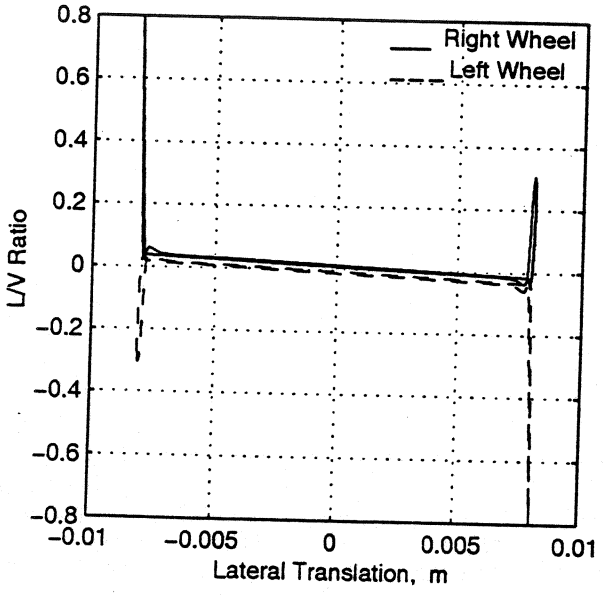

Figure 5. Wheelset L/V Ratios and Lateral Displacement (V = 30 m/sec)

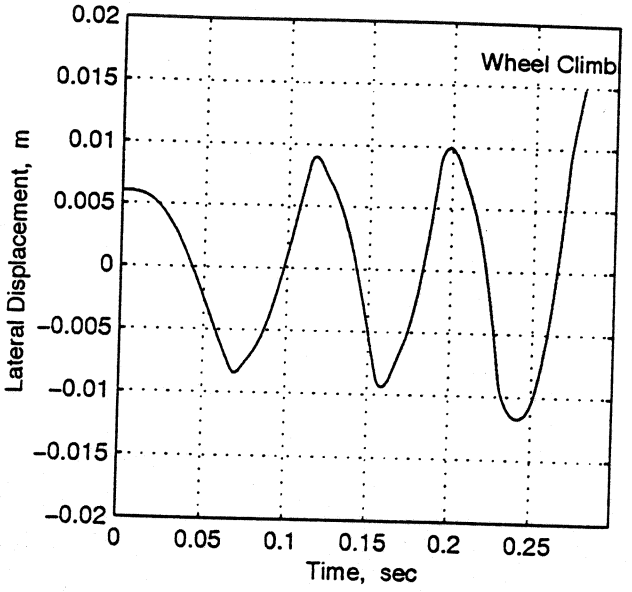

Figure 7. Wheelset Lateral Displacement Showing Wheel Climb (V = 110 m/sec, Load/Wheel = 292,410 N)

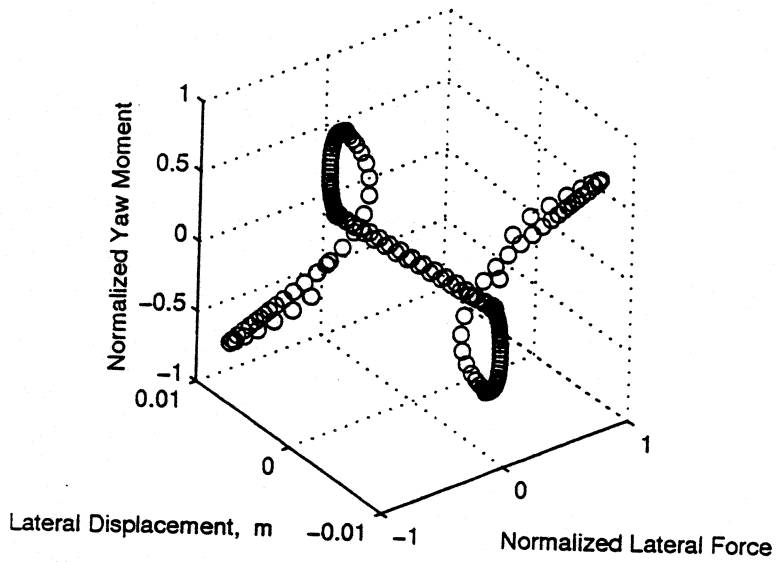

Figure 6. Effect of Flange on Lateral Force and Yaw Moment (V = 30 m/sec)

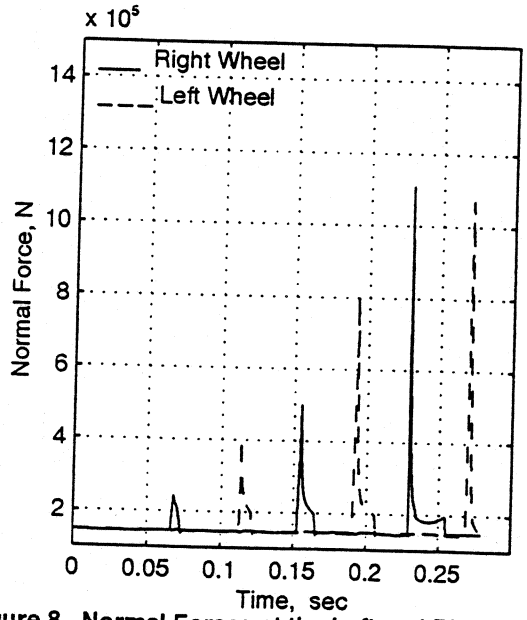

Figure 8. Normal Forces at the Left and Right Wheel (V = 110 m/sec, Load/Wheel = 292,410 N)

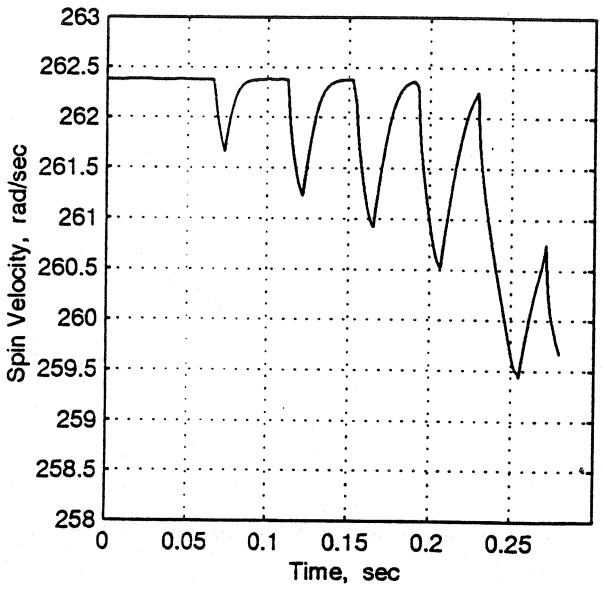

Figure 9. Wheelset Spin Rate During Wheel Climb (V = 110 m/sec, Load/Wheel = 292,410 N)

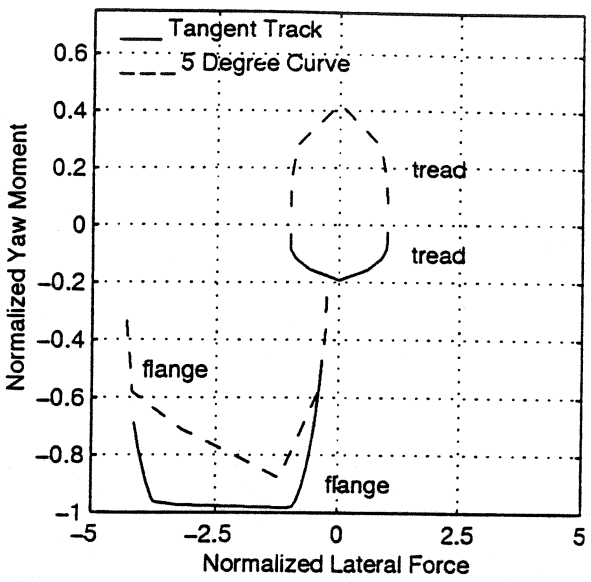

Figure 11. Normalized Lateral Force and Yaw Moment on Tread and Flange in Steady State

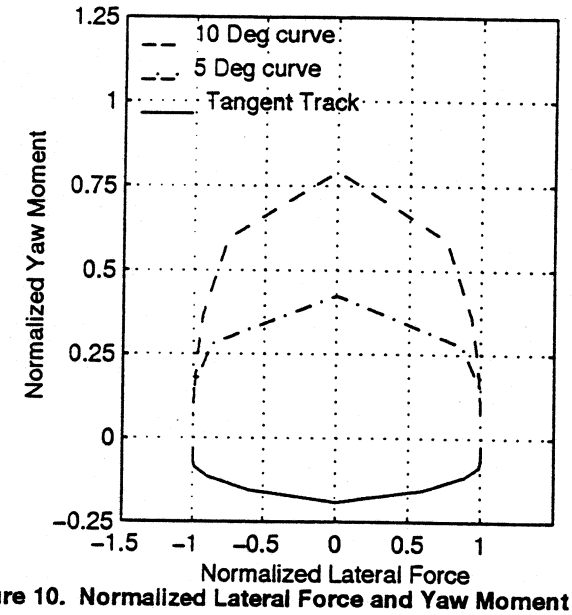

Figure 10. Normalized Lateral Force and Yaw Moment on Tread in Steady State

Table 1: Simulation Data

Wheelset Mass	1751 kg
Spin Moment of Inertia	200 kg-m^2
Yaw Moment of Inertia	761 kg-m^2
Mean Rolling Radius	0.42 m
Rail Profile	1938 N/m New Rail
Wheel Profile	AAR 1:20 New Wheel
Coefficient of Friction	0.375
Flange Clearance	0.008 m

Table 2: Stable Limit Cycle Amplitude Versus Speed

Speed m/sec	Limit Cycle Amplitude mm
30.0	8.122
27.5	8.100
25	8.079
22.5	8.061
20.0	8.044
15.0	8.020
2.0	7.900

Note: Linear critical speed for the model is 3.35 m/sec